AD-A047 086 STEVENS INST OF TECH HOBOKEN N J DEPT OF MECHANICAL --ETC F/G 1/3
RESEARCH ON THE FLUTTER OF AXIAL-TURBOMACHINE BLADING.(U)
NOV 77 F SISTO, H TOKEL N00014-76-C-0540
UNCLASSIFIED ME-RT-77004 NL

1 OF 1
AD
A047 086

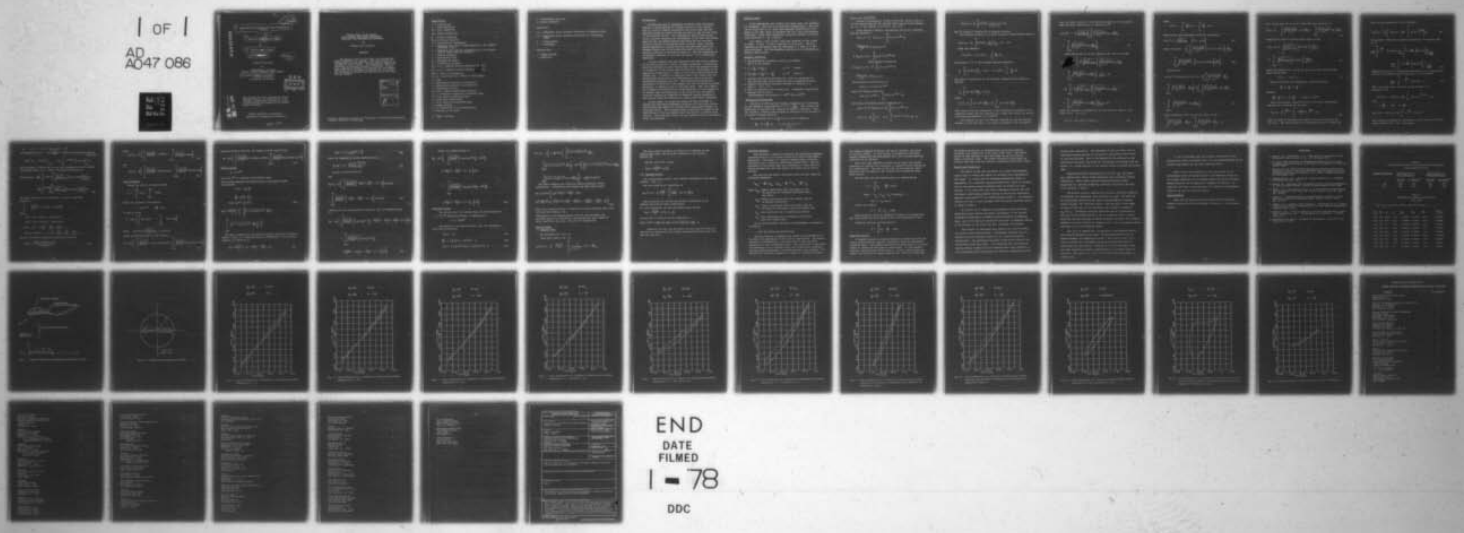

END
DATE
FILMED
1-78
DDC

(12)

(6) RESEARCH ON THE FLUTTER OF AXIAL-TURBOMACHINE BLADING

(9) Technical Report (14) ME-RT-77004

by

(10) F. Sisto and H. Tokel

(11) Nov 1977

(12) 39 p.

Research Sponsored

by

DEPARTMENT OF THE NAVY
OFFICE OF NAVAL RESEARCH, POWER BRANCH

(15) Contract N00014-76-C-0540

Project No. NR 094-363

STEVENS INSTITUTE OF TECHNOLOGY
DEPARTMENT OF MECHANICAL ENGINEERING

DYNAMIC STALL OF AN AIRFOIL WITH LEADING EDGE BUBBLE SEPARATION INVOLVING TIME DEPENDENT RE-ATTACHMENT

by

H.Tokel* and F.Sisto**

ABSTRACT

The dynamic stall of an airfoil with leading edge bubble separation is analyzed. The stall flutter of turbomachine blading often involves periodic growth and collapse of such a bubble. The mathematical model representing the physical problem is presented. A flat plate undergoing harmonic oscillations with time dependent point of re-attachment is studied for the perturbed aerodynamic reactions and applications to the stall flutter problem.

*Graduate Research Assistant and **Professor of Mechanical Engineering
Stevens Institute of Technology

Nomenclature

a = acceleration

b = blade semichord

C_L = lift coefficient

C_M = moment coefficient

$\mathcal{F}$ = Fourier transform

f, g = auxiliary functions

h = translational displacement

i = imaginary unit used in representation of the complex variables Z and ζ

j = imaginary unit used in representation of the complex form of simple harmonic function

k = reduced frequency

L = perturbation lift

M = perturbation moment

p = perturbation pressure

$R_o + j J_o$ = complex function defined by Eq. (14)

$R_1 + j J_1$ = complex function defined by Eq. (15)

$S(t)$ = point of reattachment

S_1, S_2 = upper and lower limits of reattachment

t = time

u = perturbation velocity in x-direction

v = perturbation velocity in y-direction

V = freestream velocity

$W = \phi + i\Psi$, complex acceleration potential

x, y = cartesian coordinates in physical plane

$Z = x + iy$ point in physical plane

α = rotational displacement

$\zeta = \xi + i\eta$ point in transformed plane

μ = dummy variable

ξ, η = coordinates in transformed plane

ρ = density of the fluid

$\sigma = \left|\frac{x}{2b}\right|$ a variable

ϕ = acceleration potential

χ = phase difference

Subscripts:

x,y = components along cartesian coordinates in physical plane

ξ,η = components along cartesian coordinates in transformed plane

h = translational

α = rotational

Superscripts:

' = dummy variable

$\bar{}$ = amplitude

Introduction

An important type of phenomenon classified under the general heading of aeroelasticity of lifting surfaces is stall flutter. This is a type of dynamic instability that occurs when the flow separates around an airfoil through the whole or part of each cycle of its vibratory motion. This nonclassical type of flutter may involve periodic breakaway and reattachment of the flow and various types of time lag effects between the motion and the reactions. The stall flutter of helicopter rotors, aircraft wings, aircraft engine compressors at ground start up and high speed flight are examples giving rise to non-steady flow about an airfoil and a possible condition of destructive behavior. Thus the prediction of aerodynamic reactions in such flow situations is of considerable importance.

In many instances the flow separation from the suction surface of the airfoil does not involve a complete breakaway. Particularly with thin airfoils of small leading edge radius the separation point is "anchored" at the leading edge followed by a reattachment of the separation stream line at a point on the suction surface behind the leading edge. A "bubble" of separated flow is thus formed near the leading edge within which the velocities are quite low and the perturbation pressure near zero. The detailed fluid mechanical description of the flow is very complex, but the net effect on surface pressures is substantially as described above. When the airfoils of a cascade are configured as in the compressor of a gas turbine it is thought that the channelling of the relative flow by adjacent airfoils inhibits the formation of separated regions extending to the trailing edges and promotes the leading edge bubble phenomenon.

In this paper an analytical method has been developed to predict the perturbed aerodynamic reactions of a flat plate airfoil with leading edge bubble of variable extent undergoing harmonic oscillatory motion. This technique with an empirical knowledge of the time history of the reattachment point can be used to predict stall flutter. Some numerical results and the computer plots of the dynamic loops are presented.

Physical Model

A two dimensional thin airfoil with small camber and incidence is considered. The flow is inviscid and incompressible. The problem is linear due to (i) small time dependent displacements (ii) small or zero mean angle of incidence and (iii) small perturbation velocities. Under these conditions a pressure function or acceleration potential $\phi = -\frac{1}{\rho} \cdot p$ exists.

As a model, a flat airfoil with zero thickness on the x-axis is taken. In Fig. 1 flow is parallel to the x-axis. The flow separates at the leading edge and reattaches at a point S on the suction surface. The time-dependent positions of re-attachment are shown by dotted lines.

Boundary Conditions

1. The perturbation pressure is zero in the bubble.
   ($\phi = 0$ in the cavity)
2. $v = \left(\frac{\partial}{\partial t} + V \frac{\partial}{\partial x}\right) y \qquad y = 0^- \qquad 0<x<2b$
3. $a_y = \left(\frac{\partial}{\partial t} + V \frac{\partial}{\partial x}\right)^2 y = \frac{\partial \phi}{\partial y} \qquad y = 0^+ \qquad S(t)<x<1$
4. Complex acceleration potential ($W = \phi + i\Psi$) is continuous at the trailing edge (Kutta condition) and the separation point.
5. Complex acceleration potential vanishes at infinity (i.e. $W(Z) \to 0$ as $Z \to -\infty$).
6. W(Z) is infinite at the leading edge. (Integrable singularity)
7. Harmonic Oscillations.
   (Displacements are given by $h = \bar{h} e^{jwt}$ and $\alpha = \bar{\alpha} e^{jwt}$)

Mathematical Development

The flow, airfoil and the boundary conditions are transformed by the conformal transformation $\zeta = \xi + i\eta = \sqrt{\frac{Z}{2b}}$. This reduces the difficulty in obtaining the solution of Laplace's Equation. Thus the Poincare boundary value problem is converted to the solution of a singular integral equation.

The prescribed value of $\frac{\partial \phi}{\partial \eta}$ on the ξ-axis is given by

$$\frac{\partial \phi}{\partial \eta} = 4b\, \xi \frac{\partial \phi}{\partial y} \quad \text{on} \quad -1 < \xi < 0 \text{ and } s(t) < \xi < +1, \quad \eta = 0+$$

where $s(t) = \sqrt{S(t)/(2b)}$

Fourier transformation is used to find the solution $\phi(\xi,\eta,t)$ of the Laplace Equation for the half plane problem which vanishes as $\eta \to +\infty$ and reduces to $\phi(\xi,0^+,t)$ for $\eta = 0^+$.

Using Laplace's Equation and applying the Fourier transform wrt the variable ξ

$$\Phi(m,\eta,t) = \mathcal{F}\ [\phi(\xi,\eta,t)] = \int_{-\infty}^{+\infty} \phi(\xi,\eta,t) e^{-jm\xi}\, d\xi$$

$$\frac{\partial^2 \Phi(m,\eta,t)}{\partial \eta^2} = \mathcal{F}\ [\phi_{\eta\eta}(m,\eta,t)]$$

$$\mathcal{F}\ [\phi_{\xi\xi}(\xi,\eta,t)] = \int_{-\infty}^{+\infty} \phi_{\xi\xi}(\xi,\eta,t) e^{-jm\xi}\, d\xi$$

Using partial integration

$$\mathcal{F}\ [\phi_{\xi\xi}(\xi,\eta,t)] = -m^2 \int_{-\infty}^{+\infty} \phi(\xi,\eta,t) e^{-jm\xi}\, d\xi$$

$$\frac{\partial^2 \Phi(m,\eta,t)}{\partial \eta^2} - m^2 \Phi(m,\eta,t) = 0$$

The solution of this equation is

$$\Phi(m,\eta,t) = \Phi\ (m,0,t) e^{-|m|y}$$

Using the boundary condition

$$\Phi(m,\eta,t) = e^{-|m|\eta} \left[\int_{-\infty}^{+\infty} \phi(\xi',0,t) e^{-jm\xi'}\, d\xi' \right]$$

and taking the inverse Fourier transform of Φ

$$\phi(\xi,\eta,t) = \mathcal{F}^{-1}[\Phi(m,\eta,t)] = \frac{1}{2\pi} \int_{-\infty}^{+\infty} \Phi(m,\eta,t) e^{jm\xi}\, dm$$

$$\Phi(\xi,\eta,t) = \frac{1}{2\pi} \int_{-\infty}^{+\infty} \phi(\xi',\ 0,t) \left[\int_{-\infty}^{+\infty} e^{[jm(\xi'-\xi)-|m|]}\, dm \right] d\xi'$$

$$\phi(\xi,\eta,t) = \frac{1}{\pi}\int_{-\infty}^{+\infty} \phi(\xi',0^+,t)\ \frac{\eta}{\eta^2+(\xi'-\xi)^2}\ d\xi'$$

This is Poisson's integral for a harmonic function.

The conjugate function Ψ is found using the Cauchy-Riemann equation.

$$-\Psi(\xi,\eta,t) = \frac{1}{\pi}\int_{-\infty}^{+\infty} \phi(\xi',0^+,t)\ \frac{\xi'-\xi}{\eta^2+(\xi'-\xi)^2}\ d\xi' - C(t)$$

Using the indentity

$$-\Psi(\xi,0^+,t) = -\Psi(-1,0^+,t) - \int_{-1}^{\xi} \frac{\partial\Psi}{\partial\xi'}\ d\xi'$$

and putting $\eta = 0^+$ in the previous equation results in

$$\frac{1}{\pi}\int_{-\infty}^{+\infty} \phi(\xi',0^+,t)\ \frac{d\xi'}{\xi'-\xi} - C(t) = -\Psi(-1,0^+,t) - \int_{-1}^{\xi} \frac{\partial\Psi}{\partial\xi'}\ d\xi'$$

The range of integration of the infinite integral may be reduced as follows:

$$\frac{1}{\pi}\int_{-\infty}^{+\infty} \phi(\xi',0^+,t)\ \frac{d\xi'}{\xi'-\xi} = F(\xi,t)$$

where

$$F(\xi,t) = \frac{1}{\pi}\int_{-1}^{0} \phi(\xi',0^+,t)\ \frac{d\xi'}{\xi'-\xi} + \frac{1}{\pi}\int_{s(t)}^{1} \phi(\xi',0^+,t)\ \frac{d\xi'}{\xi'-\xi}$$

This results from the assumption of zero perturbation pressure in the separation bubble and the inability of a single flat airfoil to exhibit a pressure perturbation in its wake[1].

The solution of this last integral equation for the two sections between $(-1 \to 0)$ and $(s(t) \to +1)$ which is bounded at the non-special

ends, and which satisfies the singularity condition at the leading edge and Kutta condition at the trailing is[4]

$$\phi(\xi,0^{+},t) = -\frac{1}{\pi}\sqrt{\frac{1-\xi^2}{\xi(\xi-s(t))}}\left\{\int_{-1}^{0}\sqrt{\frac{\xi'(\xi'-s(t))}{1-\xi'^2}}\,F(\xi',t)\frac{d\xi'}{\xi'-\xi}\right.$$

$$\left.+\int_{s(t)}^{+1}\sqrt{\frac{\xi'(\xi'-s(t))}{1-\xi'^2}}\,F(\xi',t)\frac{d\xi'}{\xi'-\xi}\right\} \qquad (1)$$

Substituting Eq.(1) in the expression for $-\Psi(0,\eta,t)$ yields

$$-\Psi(0,\eta,t) = \frac{1}{\pi}\int_{-1}^{0}\frac{-1}{\pi}\sqrt{\frac{1-\xi'^2}{\xi'(\xi'-s(t))}}\left[\int_{-1}^{0}\sqrt{\frac{\mu(\mu-s(t))}{1-\mu^2}}\,F(\mu,t)\frac{d\mu}{\mu-\xi'}\right.$$

$$\left.+\int_{s(t)}^{+1}\sqrt{\frac{\mu(\mu-s(t))}{1-\mu^2}}\,F(\mu,t)\frac{d\mu}{\mu-\xi'}\right]\frac{\xi'}{\eta^2+\xi'^2}\,.d\xi'$$

$$+\frac{1}{\pi}\int_{s(t)}^{+1}\frac{-1}{\pi}\sqrt{\frac{1-\xi'^2}{\xi'(\xi'-s(t))}}\left[\int_{-1}^{0}\sqrt{\frac{\mu(\mu-s(t))}{1-\mu^2}}\,F(\mu,t)\frac{d\mu}{\mu-\xi'}\right.$$

$$\left.+\int_{s(t)}^{+1}\sqrt{\frac{\mu(\mu-s(t))}{1-\mu^2}}\,F(\mu,t)\frac{d\mu}{\mu-\xi'}\right]\frac{\xi'}{\eta^2+\xi'^2}\,.d\xi'$$

where the constant of integration C(t) has been put equal to zero since $-\Psi\to 0$ as $\eta\to\infty$.

$$F(\xi,t) = -\Psi(-1,0^{+},t) + N(\xi,t) \qquad (2)$$

where

$$N(\xi) = -\int_{-1}^{\xi} \frac{\partial \Psi}{\partial \xi'}\, d\xi' = \int_{-1}^{\xi} \frac{\partial \phi}{\partial \eta}\, d\xi'$$

Substituting this expression in Eq.(1) one obtains

$$\phi(\xi,0^+,t) = \sqrt{\frac{1-\xi^2}{\xi(\xi-s(t))}} \left[F(0) + Q(\xi)\right] \tag{3a}$$

where $F(0)+Q(\xi) = -\frac{1}{\pi}\left\{\int_{-1}^{0} \sqrt{\frac{\xi'(\xi'-s(t))}{1-\xi'^2}} \left[-\Psi(-1,0^+,t)+N(\xi')\right] \frac{d\xi'}{\xi'-\xi}\right.$

$$\left. + \int_{s(t)}^{+1} \sqrt{\frac{\xi'(\xi'-s(t))}{1-\xi'^2}} \left[-\Psi(-1,0^+,t)+N(\xi')\right] \frac{d\xi'}{\xi'-\xi}\right\} \tag{3b}$$

Using Eq.(2)

$$-\Psi(-1,0^+,t)+N(0)+Q(\xi)=\Psi(-1,0^+,t) - \frac{1}{\pi}\left[\int_{-1}^{0} \sqrt{\frac{\xi'(\xi'-s(t))}{1-\xi'^2}}\, \frac{d\xi'}{\xi'-\xi}\right.$$

$$\left. + \int_{s(t)}^{+1} \sqrt{\frac{\xi'(\xi'-s(t))}{1-\xi'^2}}\, \frac{d\xi'}{\xi'-\xi}\right] - \frac{1}{\pi}\left[\int_{-1}^{0} \sqrt{\frac{\xi'(\xi'-s(t))}{1-\xi'^2}}\, N(\xi')\frac{d\xi'}{\xi'-\xi}\right.$$

$$\left. + \int_{s(t)}^{+1} \sqrt{\frac{\xi'(\xi'-s(t))}{1-\xi'^2}}\, N(\xi')\frac{d\xi'}{\xi'-\xi}\right] \tag{4}$$

Using integration over the contour shown in Fig. 1

$$\int_{-1}^{0} \sqrt{\frac{\xi'(\xi'-s(t))}{1-\xi'^2}}\, \frac{d\xi'}{\xi'-\xi} + \int_{s(t)}^{+1} \sqrt{\frac{\xi'(\xi'-s(t))}{1-\xi'^2}}\, \frac{d\xi'}{\xi'-\xi} = -\pi$$

This result when put in Eq.(4) simplifies that expression to

$$Q(\xi) = -\frac{1}{\pi} \int_{-1}^{0} \sqrt{\frac{\xi'(\xi'-s(t))}{1-\xi'^2}}\, N(\xi') \frac{d\xi'}{\xi'-\xi} + \int_{s(t)}^{+1} \sqrt{\frac{\xi'(\xi'-s(t))}{1-\xi'^2}}\, N(\xi') \frac{d\xi'}{\xi'-\xi} \tag{5}$$

Using Eq.(2) with $\xi=0$ and the above result yields

$$-\Psi(0,\eta,t) = \frac{1}{\pi} \int_{-1}^{0} \sqrt{\frac{1-\xi'^2}{\xi'(\xi'-s(t))}} \left[F(0)+Q(\xi')\right] \frac{\xi' d\xi'}{\eta^2+\xi'^2}$$

$$+ \frac{1}{\pi} \int_{s(t)}^{+1} \sqrt{\frac{1-\xi'^2}{\xi'(\xi'-s(t))}} \left[F(0)+Q(\xi')\right] \frac{\xi' d\xi'}{\eta^2+\xi'^2} \tag{6}$$

Using the identity for $-\Psi(\xi, 0^+, t)$, Eq.(2) and the expression for $N(\xi)$ reveals that

$$\bar{F}(\xi,t) = -\Psi(\xi, 0^+, t) \tag{7}$$

Assuming harmonic time dependence, the Euler equation

$$\frac{\partial v}{\partial t} + V \frac{\partial v}{\partial x} = -\frac{\partial \Psi}{\partial x}$$

becomes

$$\frac{\partial \bar{v}}{\partial x} + \frac{j\omega}{V} \bar{v} = -\frac{1}{V} \frac{\partial \bar{\Psi}}{\partial x} \qquad \text{since } v = \bar{v}\, e^{j\omega t}$$

Using the boundary condition $\bar{v}(-\infty) = 0$, the above differential equation has a solution of the form

$$\bar{v}(x,0) = -\frac{1}{V} e^{-\frac{j\omega}{V}x} \int_{-\infty}^{x} \frac{\partial \bar{\Psi}(x,0)}{x}\, e^{\frac{j\omega}{V}x}\, dx \tag{8}$$

where the path of integration is taken to lie entirely along the real axis. The above equation is integrated by parts to reduce the

order of the singularity in the integrand,

$$\bar{v}(0^+,0) = -\frac{1}{V}\left[-\bar{\Psi}(0^+,0) + \frac{j\omega}{V}\int_{-\infty}^{0^+} \bar{\Psi}(x,0)\, e^{\frac{j\omega}{V}x}\right]dx \qquad (9)$$

The boundary condition is applied just back of the leading edge, $x = 0^+$.

$$\lim_{\varepsilon\to 0}\int_{-\varepsilon}^{+\varepsilon} e^{\frac{j\omega x}{V}}\,\bar{\Psi}(x,0)\,dx = \lim_{\varepsilon\to 0}\int_{-\varepsilon}^{0}\left(1+\frac{j\omega x}{V}\right)\left[\bar{\Psi}(0,\eta,t)\right]_{\eta=+\sqrt{\left|\frac{x}{2b}\right|}} dx$$

$$+\lim_{\varepsilon\to 0}\int_{0}^{\varepsilon}\left(1+\frac{j\omega x}{V}\right)\left[\bar{\Psi}(\xi,0^+,t)\right]_{\xi=-\sqrt{\left|\frac{x}{2b}\right|}} dx \qquad (10)$$

Expressing $F(\xi,t)$ as a generalized polynomial in ξ, using Eqs.(2), (5),(6) and performing the integration, it is found that

$$\lim_{\varepsilon\to 0}\int_{-\varepsilon}^{+\varepsilon} e^{\frac{j\omega}{V}x}\,\bar{\Psi}(x,0)\,dx = 0 \qquad (11)$$

Thus, the upper limit in Eq.(9) may be changed to 0^-.
Writing $x = -|x|$

$$V\,\bar{v}(0^+,0) = -\bar{\Psi}(0^+,0) + \frac{j\omega}{V}\int_{0}^{\infty} \bar{\Psi}(x,0)\, e^{-\frac{j\omega}{V}|x|}\, d|x|$$

with

$$\sigma \equiv \frac{|x|}{2b} \qquad \text{and} \qquad k \equiv \frac{\omega b}{V}$$

$$Vv(0^+,0) = -\bar{\Psi}(0^+,0) + j2k\int_{0}^{\infty} e^{-j2k}\,\Psi(x,0)\,d\sigma$$

Now, one has to change the coordinates of the function $\bar{\Psi}$. On the lower surface $x=0^+$, $y=0^-$ corresponds

to $\xi = 0^-$, $\eta = 0^+$ and $-\infty<x<0^-$, $y=0$

corresponds to $\xi= 0$, $0<\eta= \sqrt{\left|\frac{x}{2b}\right|} <\infty$. Thus, continuing the previous reduction

$$V\bar{v}(0^+,0)= - \bar{\Psi}(\xi,0^+,t)_{\xi=0^-} + j2k \int_0^\infty e^{-j2k\sigma} \left[\bar{\Psi}\ (0,\eta,t)\right]_{\eta=\sigma} d\sigma$$

With reference to Equations (6) and (7), changing the dummy variable and substituting $\eta= \sigma$ reduces the previous equation to

$$V\bar{v}(0^+,0)=\bar{F}(0^-)-\frac{j2k}{\pi} \int_0^\infty e^{-j2k\sigma} \left\{ \int_{-1}^{0} \sqrt{\frac{1-\xi^2}{\xi(\xi-s(t))}} \left[\bar{F}(0,t)+\bar{Q}(\xi)\right] \frac{\xi d\xi}{\sigma+\xi^2} \right\} d\sigma$$

$$- \frac{j2k}{\pi} \int_0^\infty e^{-j2k\sigma} \left\{ \int_{s(t)}^{+1} \sqrt{\frac{1-\xi^2}{\xi(\xi-s(t))}} \left[\bar{F}(0,t)+\bar{Q}(\xi)\right] \frac{\xi d\xi}{\sigma+\xi^2} \right\} d\sigma \qquad (12)$$

The above function can be expressed in terms of tabulated functions

$$\int_0^\infty \frac{e^{-j2k\sigma}}{\sigma+\xi^2} d\sigma = g(2k\xi^2) - jf(2k\xi^2)$$

where

$$f(Z) = \sin Z\ Ci(Z) + \cos Z(-Si(Z))$$

$$g(Z) = \sin Z\ (-Si(Z)) - \cos Z\ Ci(Z)$$

$$-Si(Z) = \frac{\pi}{2} - Z + \frac{Z^3}{3!3} - \frac{Z^5}{5!5} + \frac{Z^7}{7!7} - \ldots.$$

$$Ci(Z)= 0.577216.....+ \ell nZ - \frac{Z^2}{2!2} + \frac{Z^4}{4!4} - \frac{Z^6}{6!6} + \ldots.$$

Eq.(12) is solved by numerical quadratures yielding

$$\bar{F}(0,t)= \frac{V\bar{v}(0^+,0)+j2k(R_1+jJ_1)}{1-j2k(R_o+jJ_o)} \qquad (13)$$

where

$$R_o+jJ_o = \frac{1}{\pi}\left\{\int_{-1}^{0}\sqrt{\frac{\xi(1-\xi^2)}{\xi-s(t)}}\;(g-jf)\,d\xi + \int_{s(t)}^{+1}\sqrt{\frac{\xi(1-\xi^2)}{\xi-s(t)}}(g-jf)\,d\xi\right\} \tag{14}$$

and

$$R_1+jJ_1 = \frac{1}{\pi}\left\{\int_{-1}^{0}\sqrt{\frac{\xi(1-\xi^2)}{\xi-s(t)}}\;\bar{Q}(\xi)\,(g-jf)\,d\xi + \int_{s(t)}^{+1}\sqrt{\frac{\xi(1-\xi^2)}{\xi-s(t)}}\;\bar{Q}(\xi)\,(g-jf)\,d\xi\right\} \tag{15}$$

Lift and Moment

Taking the lift to be positive down;

$$\bar{L} = -\int_{0}^{2b}\bar{p}\,dx - \int_{s(t)}^{2b}(-\bar{p})\,dx$$

where the conformal transformation

$$x = 2b(\xi^2-\eta^2), \qquad \frac{dx}{d\xi} = 4b\xi$$

is used to yield

$$\bar{L} = -4b\rho\left[\int_{-1}^{0}\bar{\phi}(\xi,0)\,\xi\,d\xi + \int_{s(t)}^{+1}\bar{\phi}(\xi,0)\,\xi\,d\xi\right]$$

Using $\phi(\xi,0^+,t) = \sqrt{\frac{1-\xi^2}{\xi(\xi-s(t))}}\;[F(0)+Q(\xi)]$

which was derived earlier in the analysis,

$$\bar{L} = -4b\rho\left\{\int_{-1}^{0}\sqrt{\frac{\xi(1-\xi^2)}{\xi-s(t)}}\;[F(0,t)+\bar{Q}(\xi,t)]\;d\xi + \int_{s(t)}^{+1}\sqrt{\frac{\xi(1-\xi^2)}{\xi-s(t)}}[\bar{F}(0,t)+\bar{Q}(\xi,t)]\,d\xi\right\} \tag{16}$$

Assuming positive stalling, the moment is given similarly by

$$\bar{M}= -8b^2\rho\left\{ \int_{-1}^{0} \sqrt{\frac{\xi(1-\xi^2)}{\xi-s(t)}}[\bar{F}(0,t)+\bar{Q}(\xi,t)]\xi^2 d\xi + \int_{s(t)}^{+1} \sqrt{\frac{\xi(1-\xi^2)}{\xi-s(t)}}[\bar{F}(0,t)+\bar{Q}(\xi,t)]\xi^2 d\xi \right\} \qquad (17)$$

Bending Motion

$$y= -\bar{h}\, e^{jwt}$$

Here $h=\bar{h}\, e^{jwt}$ is reckoned to be positive down.

The relevant equations derived earlier in the analysis yield successively

$$\bar{v}(0^+) = -jkV\,\frac{\bar{h}}{b}$$

$$\frac{\partial\phi}{\partial\eta} = 4b^2\omega^2\,\frac{\bar{h}}{b}\,\xi$$

$$\bar{N}(\xi)= 2b^2\omega^2\,\frac{\bar{h}}{b}\,(\xi^2-1) \qquad (18)$$

$$\bar{Q}(\xi)= \frac{2b^2\omega^2\bar{h}}{b}\left\{ \frac{1}{\pi}\left[\int_{-1}^{0} \sqrt{\xi'(\xi'-s(t))(1-\xi'^2)}\;\frac{d\xi'}{\xi'-\xi} + \right.\right.$$

$$\left.\left. + \int_{s(t)}^{+1} \sqrt{\xi'(\xi'-s(t))(1-\xi'^2)}\;\frac{d\xi'}{\xi'-\xi}\right] +1\right\}$$

The above integrals are evaluated by contour integration (contours similar to Fig. 1). When the result is substituted in the previous equation it simplifies to

$$\bar{Q}(\xi)= \frac{2b^2\omega^2\,\bar{h}}{b}\,\left(\xi^2 - \frac{s(t)\xi}{2} - \frac{s^2(t)}{8} + \frac{1}{2}\right) \qquad (19)$$

$$\bar{F}_h(0) = 2(A_h+jB_h)b^2\,\omega^2\,\frac{\bar{h}}{b} \tag{20}$$

where the subscript h denotes bending motion.

$$A_h+jB_h = j\,\frac{1}{2}\,\frac{-\frac{1}{k}+4k\,(R_2+jJ_2)}{1-j2k(R_o+jJ_o)} \tag{21}$$

R_o+jJ_o is given by Eq.(14)

and

$$R_2+jJ_2 = \frac{1}{\pi}\left\{\int_{-1}^{0}\sqrt{\frac{\xi(1-\xi^2)}{\xi-s(t)}}\left[-\frac{s(t)\,\xi}{2}-\frac{s^2(t)}{8}+\xi^2+\frac{1}{2}\right](g-jf)\,d\xi\right.$$

$$\left.+\int_{s(t)}^{+1}\sqrt{\frac{\xi(1-\xi^2)}{\xi-s(t)}}\left[-\frac{s(t)\xi}{2}-\frac{s^2(t)}{8}+\xi^2+\frac{1}{2}\right](g-jf)\,d\xi\right\} \tag{22}$$

Substituting the above results in Eq.(16), lift for bending motion is

$$\bar{L}_h = -4b\rho\left\{\int_{-1}^{0}\sqrt{\frac{\xi(1-\xi^2)}{\xi-s(t)}}\cdot\left[2(A_h+jB_h)b^2\,2\frac{\bar{h}}{b}+\frac{2b^2\omega^2\bar{h}}{b}\left[-\frac{s(t)\,\xi}{2}-\frac{s^2(t)}{8}+\xi^2+\frac{1}{2}\right]\right]d\xi\right.$$

$$\left.+\int_{s(t)}^{+1}\sqrt{\frac{\xi(1-\xi^2)}{\xi-s(t)}}\left[2(A_h+jB_h)b^2\omega^2\frac{\bar{h}}{b}\cdot\right.\right.$$

$$\left.\left.+\frac{2b^2w^2\bar{h}}{b}\left[-\frac{s(t)\,\xi}{2}-\frac{s^2(t)}{8}+\xi^2+\frac{1}{2}\right]\right]d\xi\right\} \tag{23}$$

Moment for bending motion is

$$\bar{M}_h = -8b^2\rho\left\{ \int_{-1}^{0} \sqrt{\frac{\xi(1-\xi^2)}{\xi - s(t)}} \left[2(A_h + jB_h) b^2\omega^2 \frac{\bar{h}}{b} + 2b^2\omega^2 \frac{\bar{h}}{b} \right.\right.$$

$$\left. \left[-\frac{s(t)\,\xi}{2} - \frac{s^2(t)}{8} + \xi^2 + \frac{1}{2} \right] \right] \xi^2 d\xi$$

$$+ \int_{s(t)}^{+1} \sqrt{\frac{\xi(1-\xi^2)}{\xi - s(t)}} \left[2(A_h + jB_h) b^2\omega^2 \frac{\bar{h}}{b} + 2b^2\omega^2 \frac{\bar{h}}{b} \right.$$

$$\left.\left. \left[-\frac{s(t)\,\xi}{2} - \frac{s^2(t)}{8} + \xi^2 + \frac{1}{2} \right] \right] \xi^2 d\xi \right\} \qquad (24)$$

Torsional Motion

For torsion about the leading edge, the displacement for $\alpha = \bar{\alpha}\, e^{jwt}$ positive stalling, is expressed as

$$y = -\bar{\alpha} x e^{jwt}$$

Analogously to the bending motion case, the expressions are given successively

$$\bar{v}(0^+) = -v\bar{\alpha} \qquad (25)$$

$$\frac{\partial \bar{\phi}}{\partial \eta} = \left[-j\,\frac{8}{k}\, b^2\omega^2\xi + 8b^2\omega^2\xi^3 \right] \bar{\alpha} \qquad (26)$$

$$\bar{N}(\xi) = \left[-j\,\frac{4}{k}\, b^2\omega^2(\xi^2 - 1) + 2b^2\omega^2(\xi^4 - 1) \right] \bar{\alpha} \qquad (27)$$

$$\bar{Q}(\xi,t)= -\frac{1}{\pi}\Bigg\{ -(-j\frac{4}{k}b^2\omega^2)\bar{\alpha}\Bigg[\int_{-1}^{0}\sqrt{\xi'(\xi'-s(t))(1-\xi'^2)}\ \frac{d\xi'}{\xi'-\xi}$$

$$\int_{s(t)}^{+1}\sqrt{\xi'(\xi'-s(t))(1-\xi'^2)}\ \frac{d\xi'}{\xi'-\xi}\Bigg] -2b^2\omega^2\bar{\alpha}\Bigg[\int_{-1}^{0}\sqrt{\xi'(\xi'(\xi'-s(t))(1-\xi'^2)}(1+\xi'^2)\frac{d\xi'}{\xi'-\xi}$$

$$\int_{s(t)}^{+1}\sqrt{\xi'(\xi'-s(t))(1-\xi'^2)}\,(1+\xi'^2)\frac{d\xi'}{\xi'-\xi}\Bigg]\Bigg\} -j\frac{4}{k}b^2\omega^2\bar{\alpha}+2b^2\omega^2\bar{\alpha}$$

The above integrals are solved by similar elaborate contour integrations. Substituting the results and after some algebra,

$$\bar{Q}(\xi,t)=b^2\omega^2\bar{\alpha}\Bigg\{-j\frac{4}{k}\Big[\xi^2-\frac{s(t)\ \xi}{2}-\frac{s^2(t)}{8}+\frac{1}{2}\Big]+2$$

$$\Big[\xi^4-\frac{s(t)-\xi^3}{2}+\Big(\frac{1}{2}-\frac{s^2(t)}{8}\Big)\xi^2+\Big(\frac{-s(t)}{4}-\frac{s^3(t)}{16}\Big)\xi-\frac{5-s^4(t)}{128}-\frac{s^2(t)}{16}+\frac{3}{8}\Big]\Bigg\} \qquad (28)$$

$\bar{F}(0,t)$ for torsional Motion is obtained by substituting Eqs.(25), (14), (15) and (28) into Eq. (13).

Analogously to the bending motion, the lift and the moment for torsional motion are obtained by substituting the above values of $\bar{Q}(\xi,t)$ and $\bar{F}(0,t)$ into Eqs. (16) and (17) respectively.

Special Cases:

(i) Attached Flow:

For Attached Flow $s(t) = 0$.

Using this value in Eq. (1)

$$\phi(\xi,0^+,t)= -\frac{1}{\pi}\ \frac{\sqrt{1-\xi^2}}{\xi}\ \int_{-1}^{+1}\frac{\xi'}{\sqrt{1-\xi'^2}}\ F(\xi')\ \frac{d\xi'}{\xi'-\xi}$$

The above result satisfies the singularity condition at the leading edge ($\xi=0$), and the Kutta condition at the trailing edge($\xi= \pm 1$).

Eq.(19) with s(t)= gives

$$\bar{Q}(\xi)= \frac{2\, b^2\omega^2\bar{h}}{b}\ (\xi^2+\frac{1}{2})$$

(ii) Stalled Airfoil:

For an oscillating airfoil with complete separation on the suction surface $s(t) = 1$.

For this value Eq.(1) simplifies to

$$\phi(\xi,0^+,t)= -\frac{1}{\pi}\sqrt{\frac{1+\xi}{-\xi}}\int_{-1}^{0}\sqrt{\frac{-\xi'}{1+\xi'}}\ F(\xi',t)\ \frac{d\xi'}{\xi'-\xi}$$

This satisfies the singularity and Kutta conditions at the leading and trailing edges respectively.

For full separation, Eq.(19) of bending motion becomes

$$\bar{Q}(\xi)= \frac{2b^2\omega^2\bar{h}}{b}\ (\xi^2-\frac{1}{2}\ \xi + \frac{3}{8})$$

and Eq.(28) of torsional motion simplifies to

$$\bar{Q}(\xi)= b^2\omega^2\bar{\alpha}\ [-j\frac{4}{k}(\xi^2-\frac{1}{2}\ \xi+\frac{3}{8})+2(\xi^4-\frac{1}{2}\ \xi^3+\frac{3}{8}\xi^2-\frac{5}{16}\ \xi+\frac{35}{128}\ .)]$$

Similarly the lift and the moment for these special cases are obtained by substituting the relevant expressions derived above into Eqs.(16) and (17).

Stability Analysis

This analysis is aimed at predicting the perturbed aerodynamic characteristics of a flat plate airfoil with leading edge bubble separation. The motion is a harmonic bending and/or torsional oscillation in an otherwise undisturbed uniform field. The flow separates at the leading edge and reattaches at a point which is moving periodically with time between two limits on the suction surface.

One can find the moment coefficient about any axis using the following expression.

$$C_{M_{\alpha x}} = -\left(\frac{x}{2b}\right) C_{M_{h0}} + C_{M_{\alpha 0}} + \left(\frac{x}{2b}\right)^2 C_{L_h} - \left(\frac{x}{2b}\right) C_{L_h}$$

where $C_{M_{\alpha x}}$ = moment coefficient about any point x along the chord due to torsional oscillation about this point.

$C_{M_{h0}}$ = moment coefficient about the leading edge due to bending oscillation.

$C_{M_{\alpha 0}}$ = moment coefficient about the leading edge due to torsional oscillation about the leading edge.

C_{L_h} = lift coefficient due to bending oscillation.

C_{L_α} = lift coefficient due to torsional oscillation about the leading edge.

In the above analysis, the point of reattachment is assumed to be given by

$$S(t) = \frac{1}{2}\left[S_1+S_2)+(S_1-S_2)\cos(\omega t-\chi)\right]$$

The only obstacle to applying the method is the definition of the exact time dependency of the point of reattachment. The present technique is semiempirical in the sense that it uses the above expression for the reattachment point. This empiricism in specifying the expression can be improved using flow visualization techniques and high speed photography or detailed boundary layer analysis. The variation of this point depends on a number of variables including

the reduced frequency of motion, the airfoil geometry, the nature of the flow pattern. If this history is analyzed for different reduced frequencies from experimental data, more suitable empirical functions can be obtained.

Given this time dependent movement of the point, the present technique can indicate the occurrence or absence of stall flutter for any configuration. The sign of the value of work done per cycle, positive, zero or negative, will indicate this information about stall flutter.

The work done for pure bending motion is represented by

$$W \sim \int_0^{2\pi} C_{L_h} \cdot \frac{dh}{dt} \cdot d(\omega t)$$

where $C_{L_h} = C_{L_0} + C_{L_1} \cos(\omega t + \phi_1) + \ldots$

and $h = h_0 \cos \omega t$

Taking the integral

$$W \sim -\frac{1}{2} \pi C_{L_1} \cdot \sin\phi_1$$

Some numerical values are presented in Table 2 as examples for the coefficients and phase angles of the "Lift Coefficient" term

Similarly for pure torsional motion

$$W \sim \int_0^{2\pi} C_M \cdot \frac{d}{dt} \cdot d(\omega t)$$

Numerical Results

A computer program has been developed to calculate the lift and moment coefficients by numerical integration using the expressions presented above. The program calculates the coefficients at a certain number of points for each cycle of oscillation. It uses harmonic analysis, and finds the coefficients of Fourier series which represents the lift and the moment coefficients. The work coefficient

for bending oscillation is represented by one of these Fourier constants, the coefficient of the first "sine" term. The Fourier series is then employed to plot the graphs of the lift and the moment coefficient loops. The graphs presented in this paper are directly obtained using this computer program and the plotter output.

Results and Conclusions

The effect on the lift and moment of a single nonstationary airfoil with a leading edge bubble of variable extent described in this paper. To verify that the developed mathematical model is applicable, fully separated (supercavitated) flow, which is a special case of the general method presented above, is studied for this purpose. It is found that the general expressions derived for lift and moment coefficients simplify exactly to the results obtained by previous investigators[2] for supercavitating airfoils. The numerical results are also, in good agreement with the results obtained earlier as shown in Table 1.

An initial set of numerical and graphical results have been obtained for pure bending (plunging) oscillations of the airfoil. Although the discussion is based on these necessarily preliminary data, many of the physical conclusions carry over to expected results to be obtained in the future for pure torsional oscillations.

The location of the bubble that forms on the airfoil governs the airfoil stall characteristic. Aerodynamic reactions vary in a periodic but non-sinusoidal manner for an airfoil oscillating harmonically. The hysteresis increases as the travel range of the reattachment point gets wider. It is believed that the numerical results deviate somewhat from the mathematically exact solution if the reattachment point approaches the immediate neighborhood of the

leading edge singularity. The amplitudes of lift and moment due to oscillation become smaller as the point of reattachment moves closer to the trailing edge. This is attributable to the reduction of the perturbation pressure, and hence the contribution to unsteady lift and moment, of a larger portion of the suction surface including the leading edge.

Damping derivatives (imaginary part of lift, C_{Lh}, and moment $C_{M\alpha}$, coefficients) attain larger magnitudes with increasing reduced frequencies. These higher reduced frequencies produce higher amplitudes for unsteady aerodynamic reactions in general, see Figs. 6,7,8 and Figs. 9 and 10.

The present analysis supplies the necesary information required to determine the aerodynamic work including its sign. The work can be analytically obtained by the cyclic integrals $\oint Ldh$ for bending motion and $\oint Md\alpha$ for torsional motion. From the type of data shown in Table 2 this work can be calculated and is found to depend on C_{L1} and ϕ_1. Aerodynamic work per cycle may also be interpreted as the area of the closed figures in the L, h plane or the M, α plane. Work done per cycle depends on reduced frequency and phase lag of bubble movement as can be inferred by comparing Figs. 3 to 6 for phasing effect and Figs. 6 to 8 for frequency effect.

Fig. 11 is an example for a fixed point of reattachment showing the expected elliptical lift loop. The hysteresis effects due to bubble movement are emphasized in Figs. 7 and 9 and in Figs. 8,10, and 12 in which the reattachment point moves during the cycle of oscillation for each series. Crossing of the lift and moment loops has been reported by previous investigators as a possible effect of stalling. See Figs. 3, 4, 5 and 13, the last being one example of a moment loop.

It can be concluded that the integral formulation of the mathematical model as presented here is a good representation of the leading edge bubble for the cases discussed above.

With a better understanding of the time history of the reattachment point and perhaps using a time dependent phase lag, the present technique can be studied further and using a suitable mapping function can be applied for cascades of airfoils. An important next step is the execution of a numerical and graphical study of the case of torsional motion.

Acknowledgement

This work was supported by the Office of Naval Research contract N00014-76-C-0540 with James R. Patton, Jr., as a program manager.

References

1. Dowell, E.H. and Ventres, C.S., "Derivation of Aerodynamic Kernel Functions", AIAA Journal, v.11, n.11, November 1973.

2. F. Sisto "The Derivation of Aerodynamic Coefficients of a Fully Stalled Oscillating Airfoil by the method of Acceleration Potential" (unpublished)

3. Perumal, P.V.K. "The Perturbed Aerodynamic Characteristics of an Oscillating Airfoil with Time Dependent Point of Separation by the Method of Acceleration Potential", M.E. Thesis, Stevens Institute of Technology, 1972.

4. Muskhelishvili, N.I., "Singular Integral Equations", P. Noordhof, Groningen, Holland, 1953.

5. Martin, M., "Unsteady Lift and Moment on Fully Cavitating Hydrofoils at Zero Cavitation Number" Journal of Ship Research, June 1962.

6. Woods, L.C., "Aerodynamic Forces on an Oscillating Aerofoil Fitted with a Spoiler", Proc. Roy. Soc. London, Series A, No.239, 1957, pp. 328-337.

7. Sisto, F., "Linearized Theory of Nonstationary Cascades at Fully Stalled or Supercavitated Conditions", ZAMM 47, Heft 8, 1967, pp. 531-542.

8. Gakhov, F.D. "Boundary Value Problems". Translated by I.N. Sneddon, International Series of Monographs in Pure and Applied Mathematics, Pergamon Press, 1966.

9. Mikhlin, S.G., "Integral Equations and their applications to problems in Mechanics etc." Translated by A.H. Armstrong. Pergamon Press 1957.

10. Abramowitz and Stegun, "Handbook of Mathematical Functions" Dover Publications, 1964.

Table 1

Fixed Separation Point in Translational Oscillation

(Fully Separated Case)

Reduced frequency	Imaginary Part of Lift Coefficient		Imaginary Part of Moment Coefficient	
	Present	L.C.Woods[6]	Present	L.C.Woods[6]
.04	.061	.062	.019	.019
.64	.949	.965	.292	.302

Table 2

Translational (Bending) Oscillation

$h=h_o \cos\omega t$

$$C_L = C_{Lo} + C_{L1} \cos(\omega t+\phi_1) + C_{L2} \cos(\omega t+\phi_2) + \cdots\cdots\cdots$$

S_1	S_2	k	x	C_{Lo}	C_{L1}	ϕ_1	C_{L2}/C_{L1}
1/3	1/9	0.05	$-\Pi/2$	-0.01183	0.23960	-88.5	0.04967
1/3	1/9	0.05	$-\Pi/3$	0.00986	0.23949	-88.4	0.04938
1/3	1/9	0.1	$-\Pi/2$	0.02480	0.46954	88.7	0.05385
1/3	1/9	0.2	$-\Pi/2$	-0.05422	0.84945	82.7	0.06574
1/3	1/9	0.5	$-\Pi/2$	-0.10274	1.29881	83.6	0.08603
2/9	1/9	0.05	$-\Pi/2$	-0.00581	0.25164	-88.3	0.023268
2/9	1/9	0.1	$-\Pi/2$	-0.01222	0.49446	89.3	0.02559
2/9	1/9	0.2	$-\Pi/2$	-0.02801	0.9009	84	0.0323
2/9	1/9	0.5	0	0.16037	1.38703	85.6	0.04256

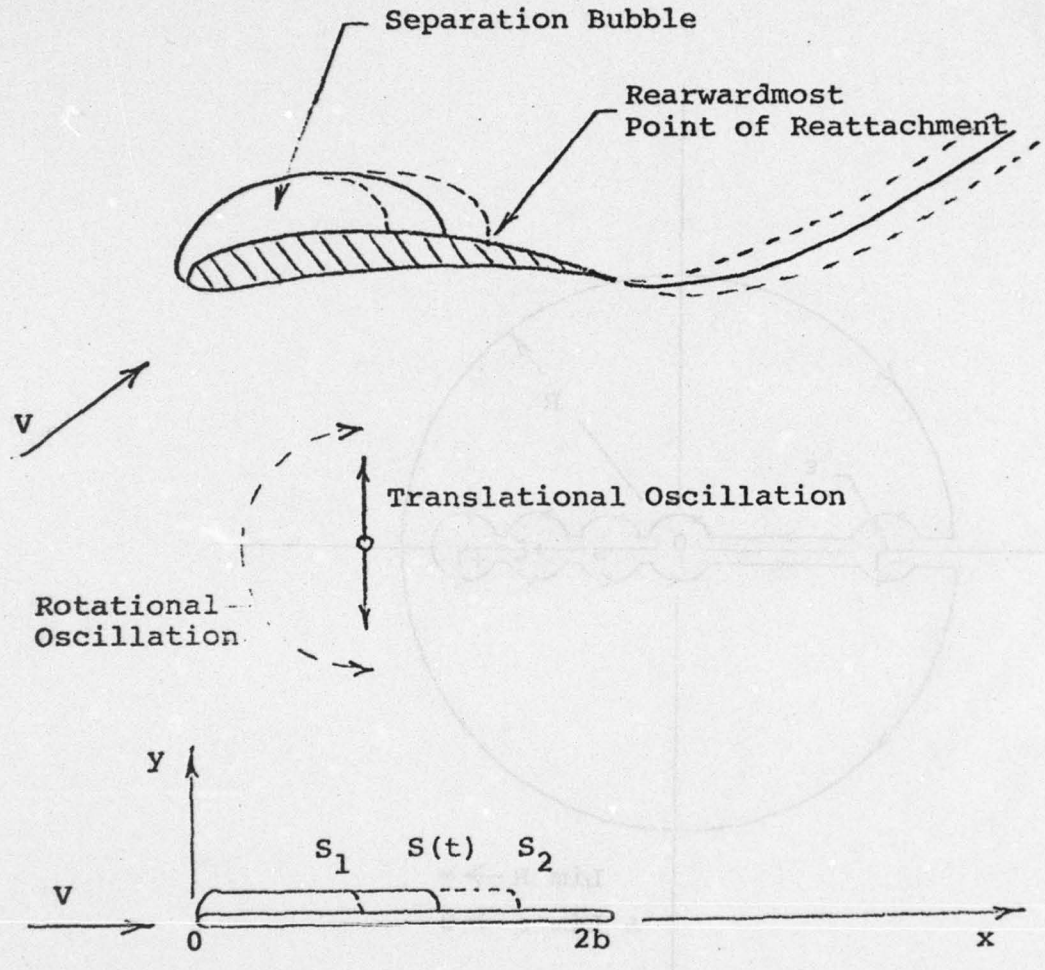

Fig. 1 - Physical model and corresponding mathematical model.

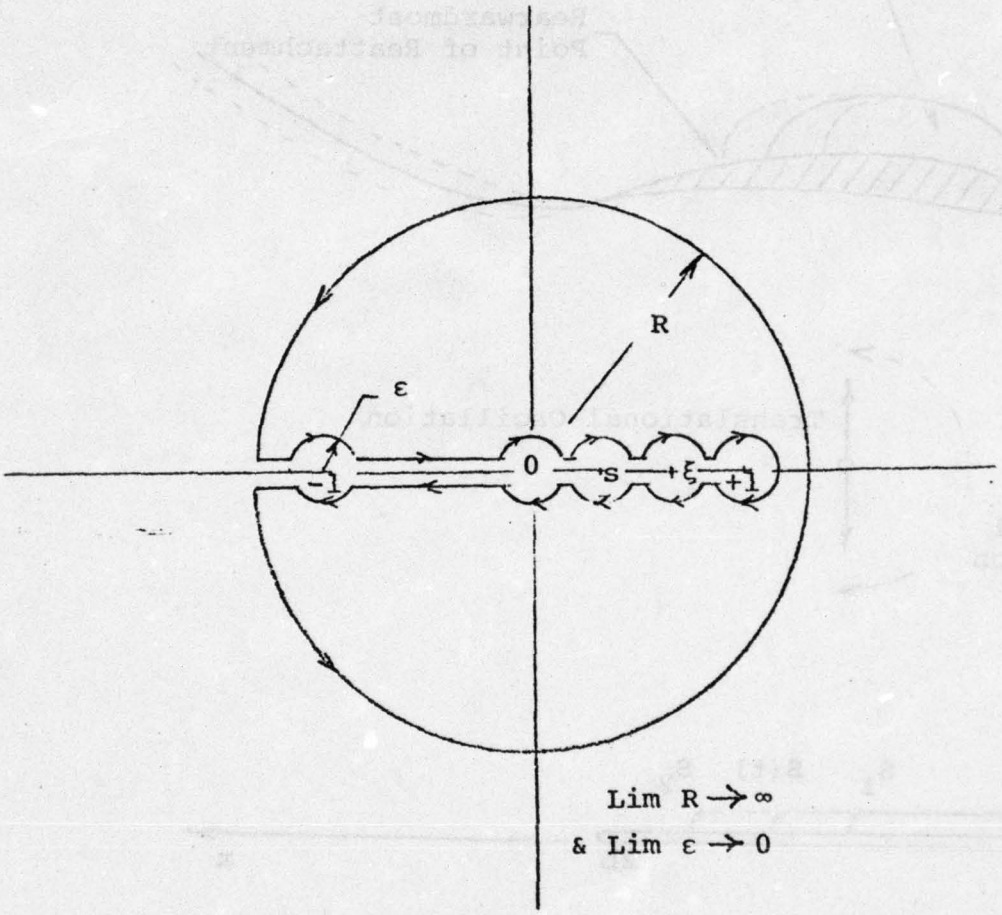

Fig. 2 - Countour for integration of Eq.(4).

$S_1 = 1/3$ $K = 0.1$

$S_2 = 1/9$ $x = 0$

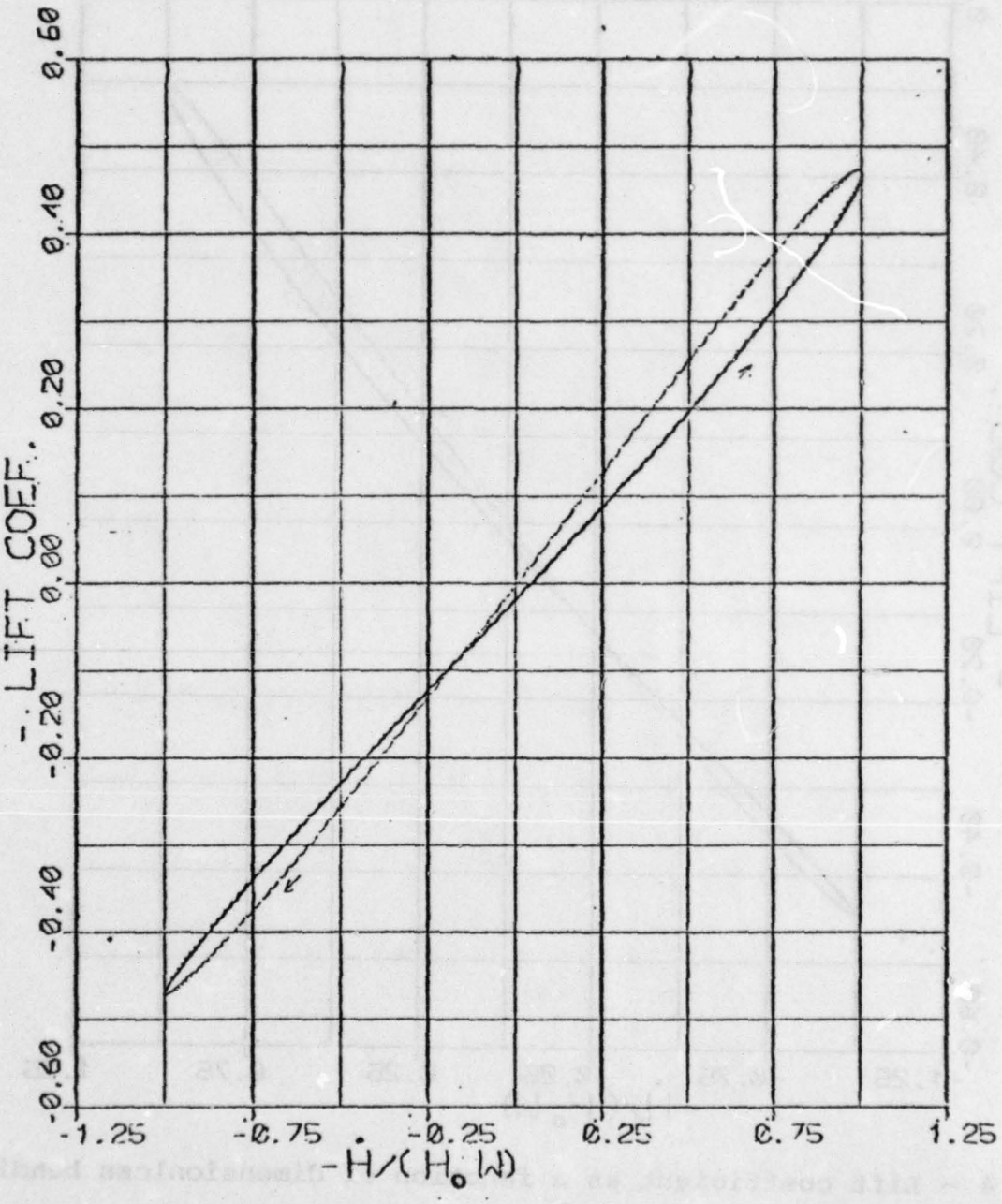

Fig. 3 - Lift coefficient as a function of dimensionless bending velocity at x = 0.

$S_1 = 1/3$ $K = 0.1$

$S_2 = 1/9$ $\chi = -\pi/6$

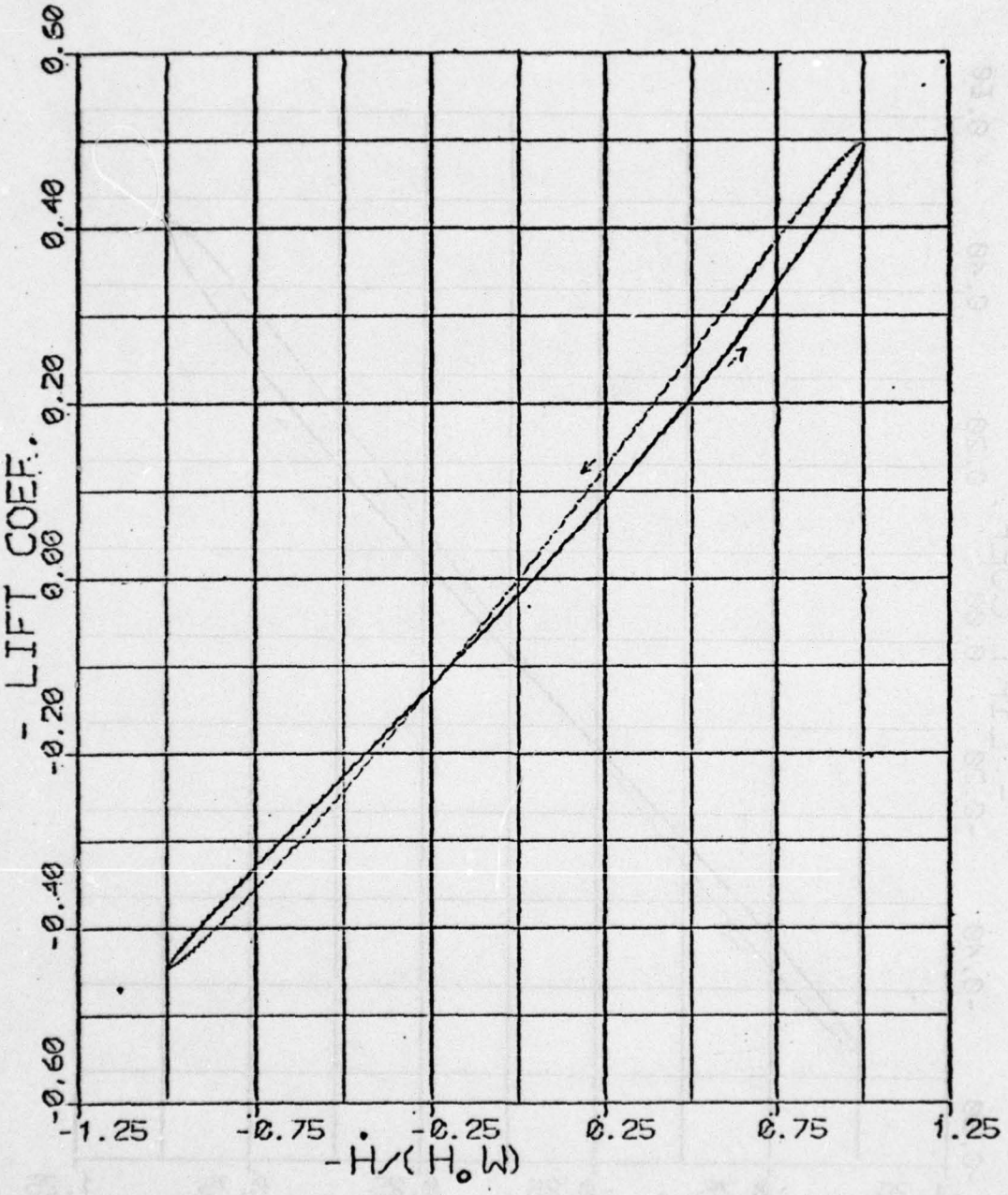

Fig. 4 - Lift coefficient as a function of dimensionless bending velocity at $x = \pi/6$.

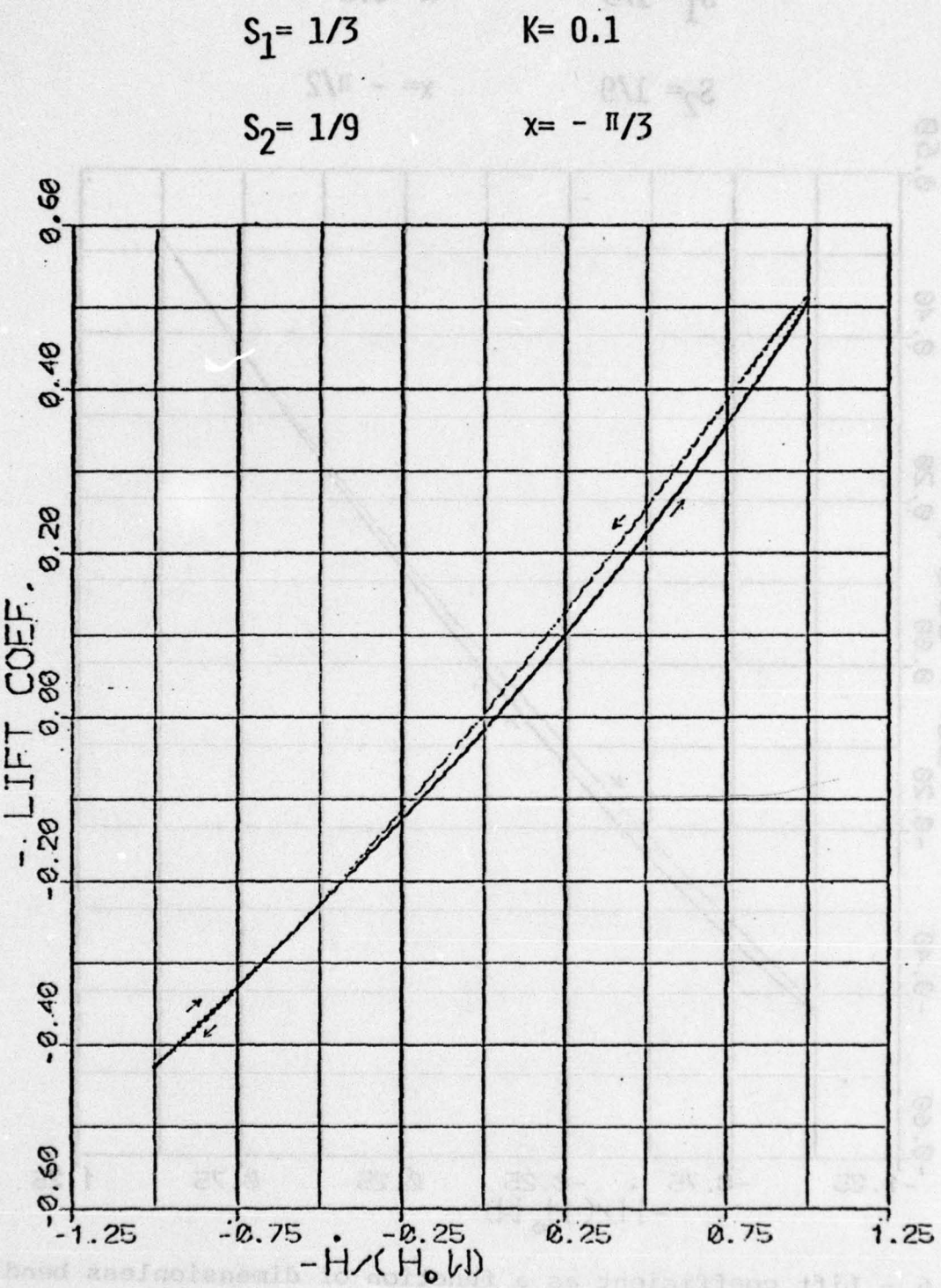

Fig. 5 - Lift coefficient as a function of dimensionless bending velocity at x = π/3.

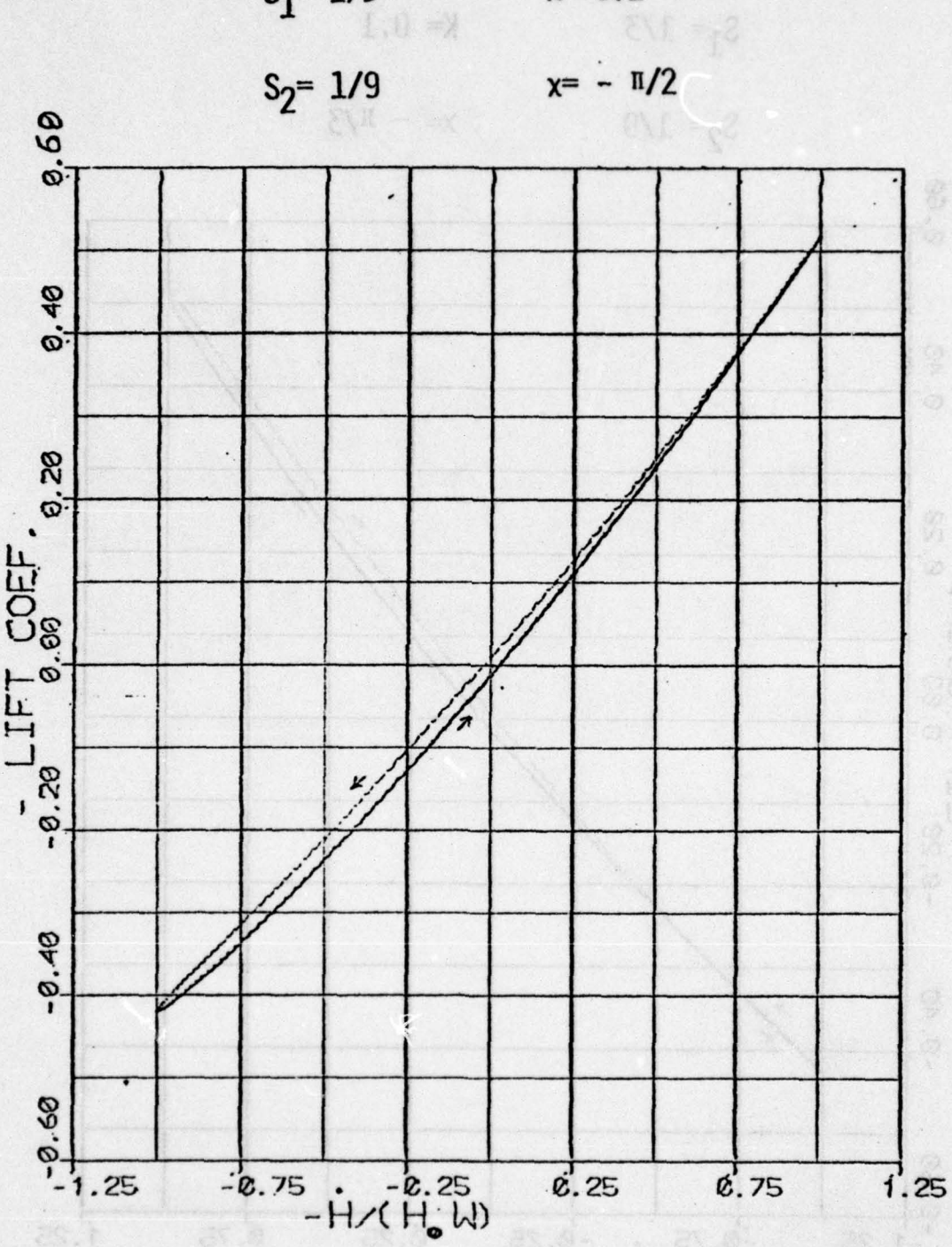

Fig. 6 - Lift coefficient as a function of dimensionless bending velocity at x = - π/2 and k = 0.1

$S_1 = 1/3$ $K = 0.2$

$S_2 = 1/9$ $x = -\pi/2$

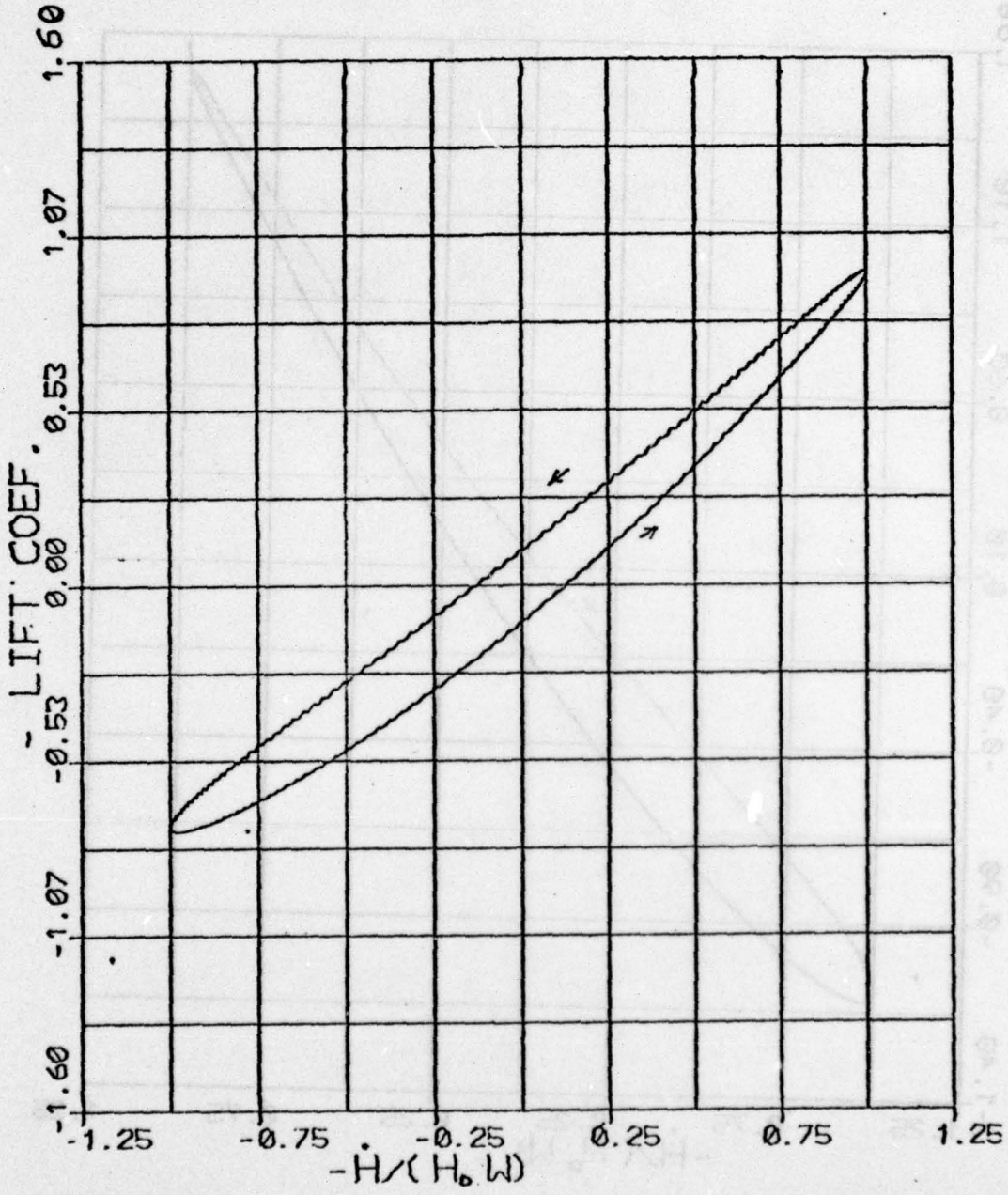

Fig. 7 - Lift coefficient as a function of dimensionless bending velocity at $x = -\pi/2$ and $k = 0.2$

$S_1 = 1/3$ $K = 0.5$

$S_2 = 1/9$ $x = -\pi/2$

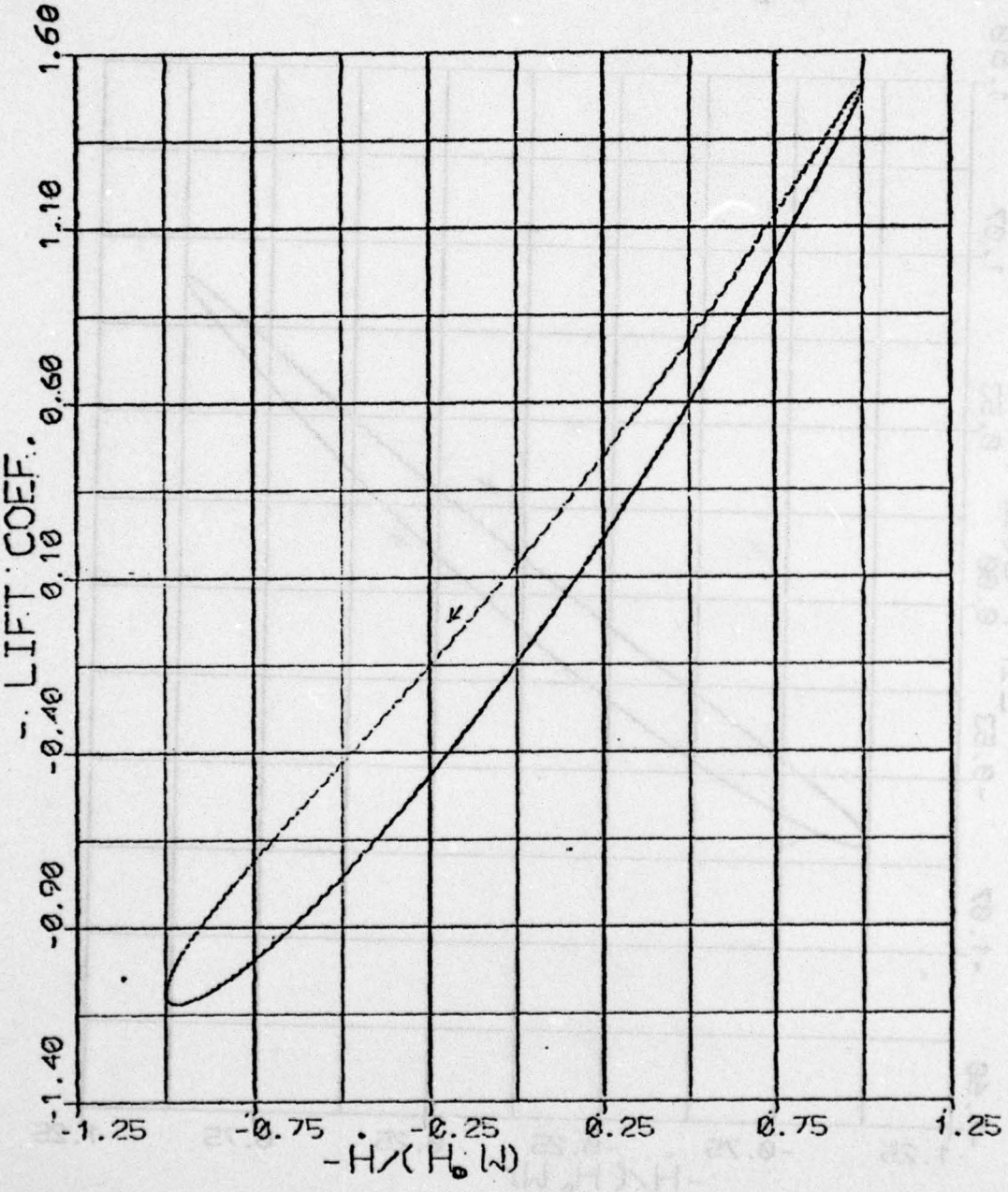

Fig. 8 - Lift coefficient as a function of dimensionless bending velocity at $x = -\pi/2$ and $k = 0.5$

$S_1 = 2/9$ $K = 0.2$

$S_2 = 1/9$ $x = -\pi/2$

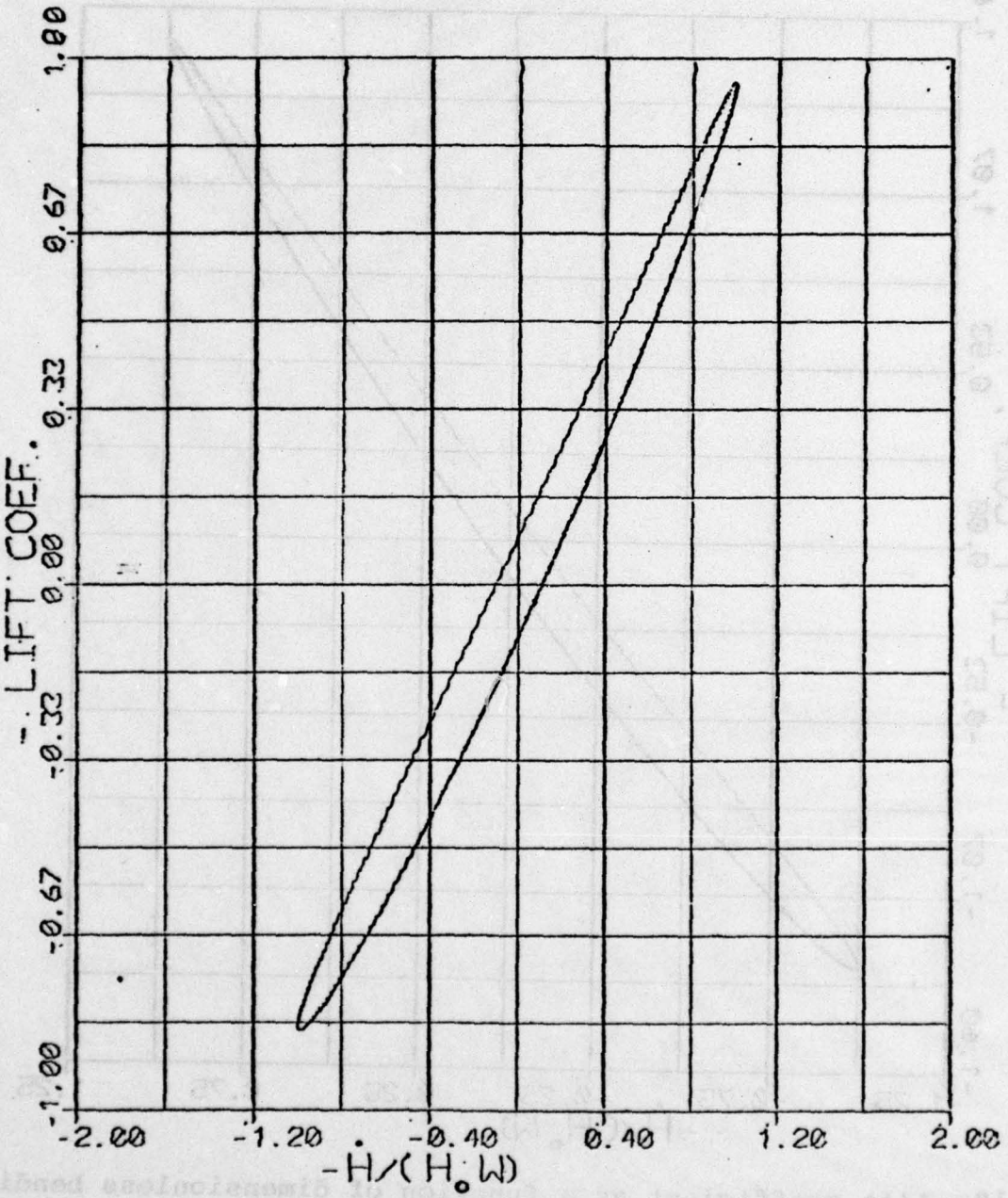

Fig. 9 - Lift coefficient as a function of dimensionless bending velocity with different reattachment point movement as compared to figure 7.

$S_1 = 2/9$ $K = 0.5$

$S_2 = 1/9$ $x = -\pi/2$

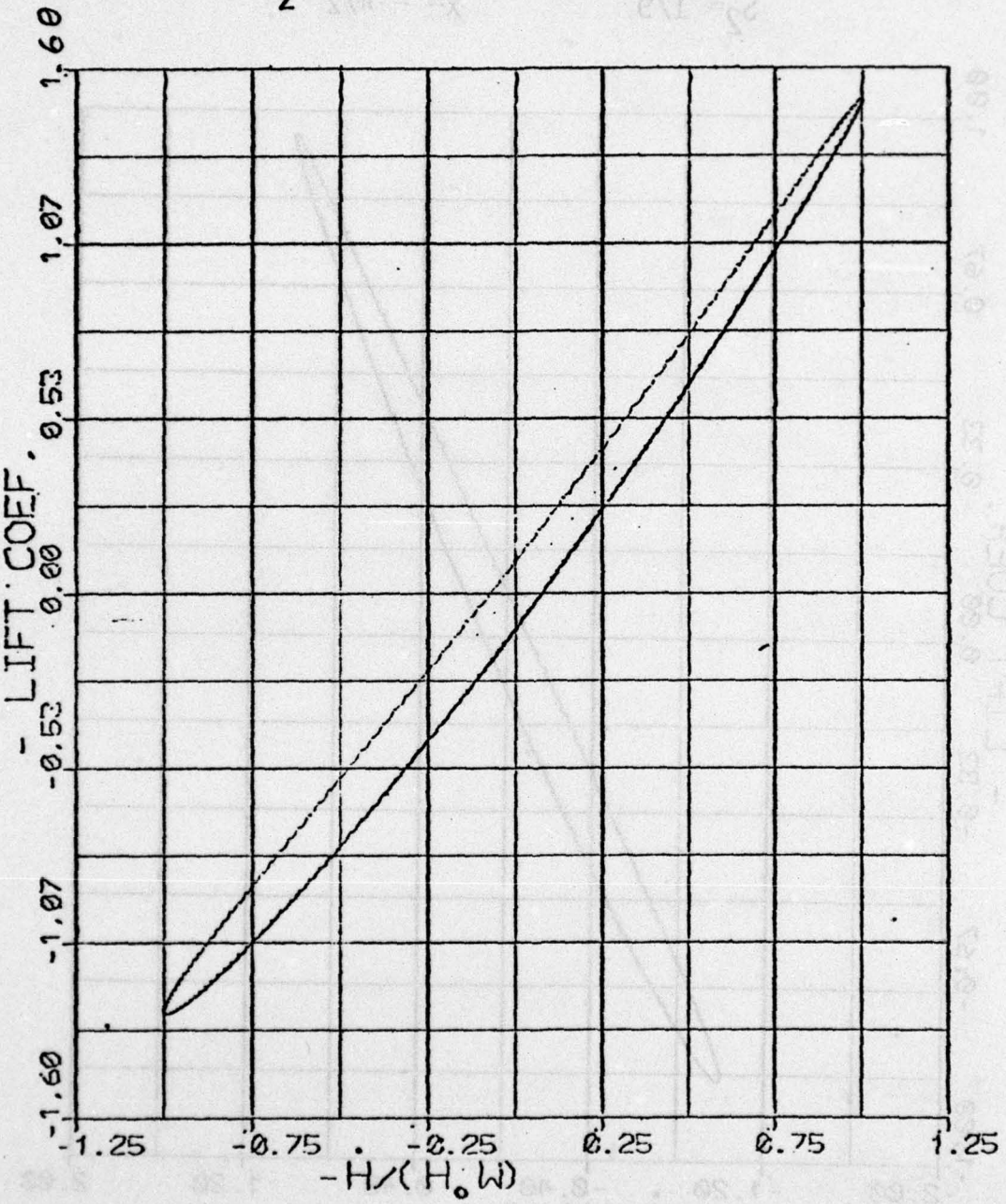

Fig. 10 - Lift coefficient as a function of dimensionless bending velocity with different reattachment point movement as compared to figure 8.

$S_1 = 1/3$ $K = 0.5$

$S_2 = 1/3$ $x =$ UNDEFINED

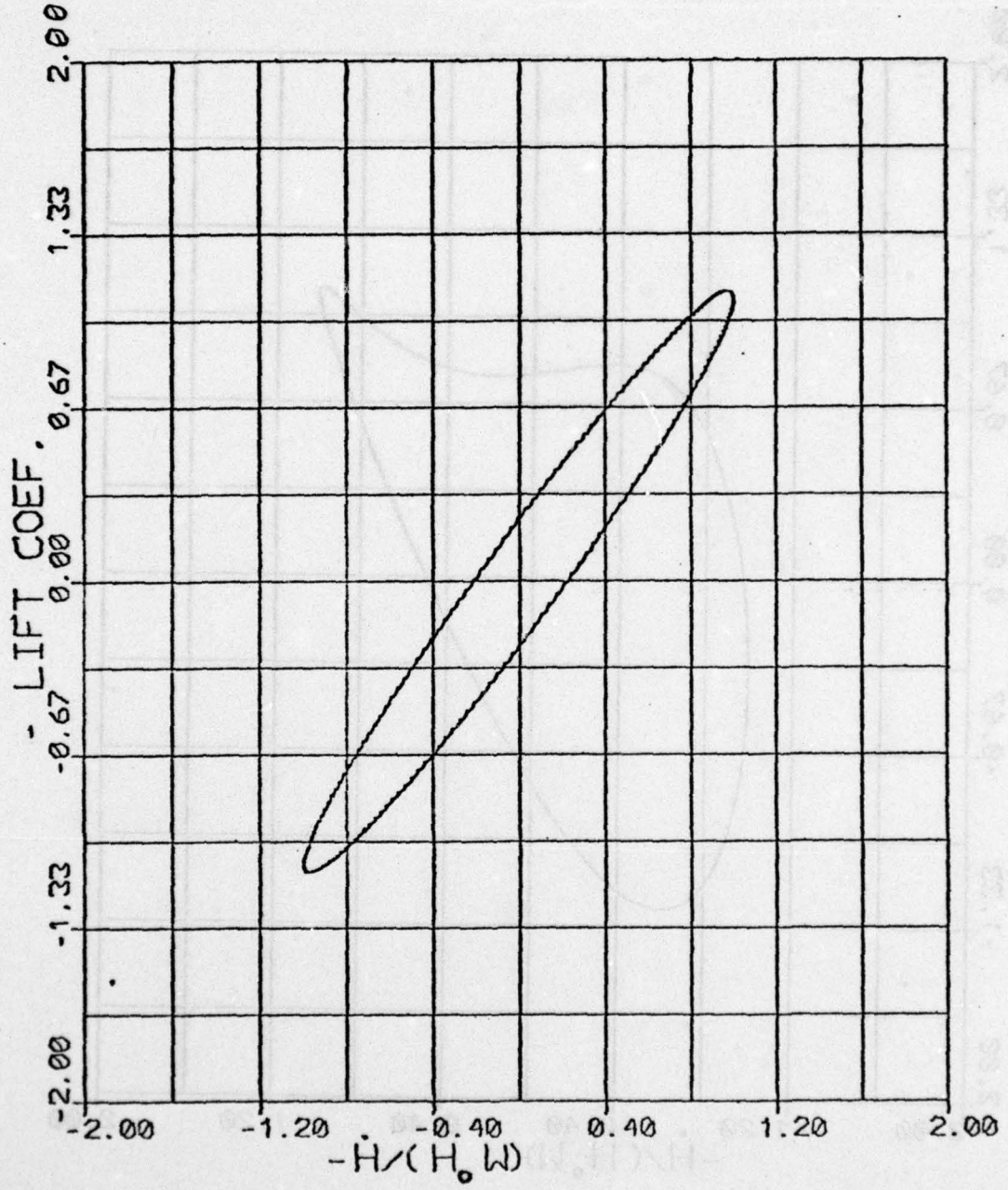

Fig. 11 - Lift coefficient as a function of dimensionless bending velocity with fixed reattachment point.

$S_1 = 1$ $K = 0.5$

$S_2 = 1/3$ $x = -\pi/2$

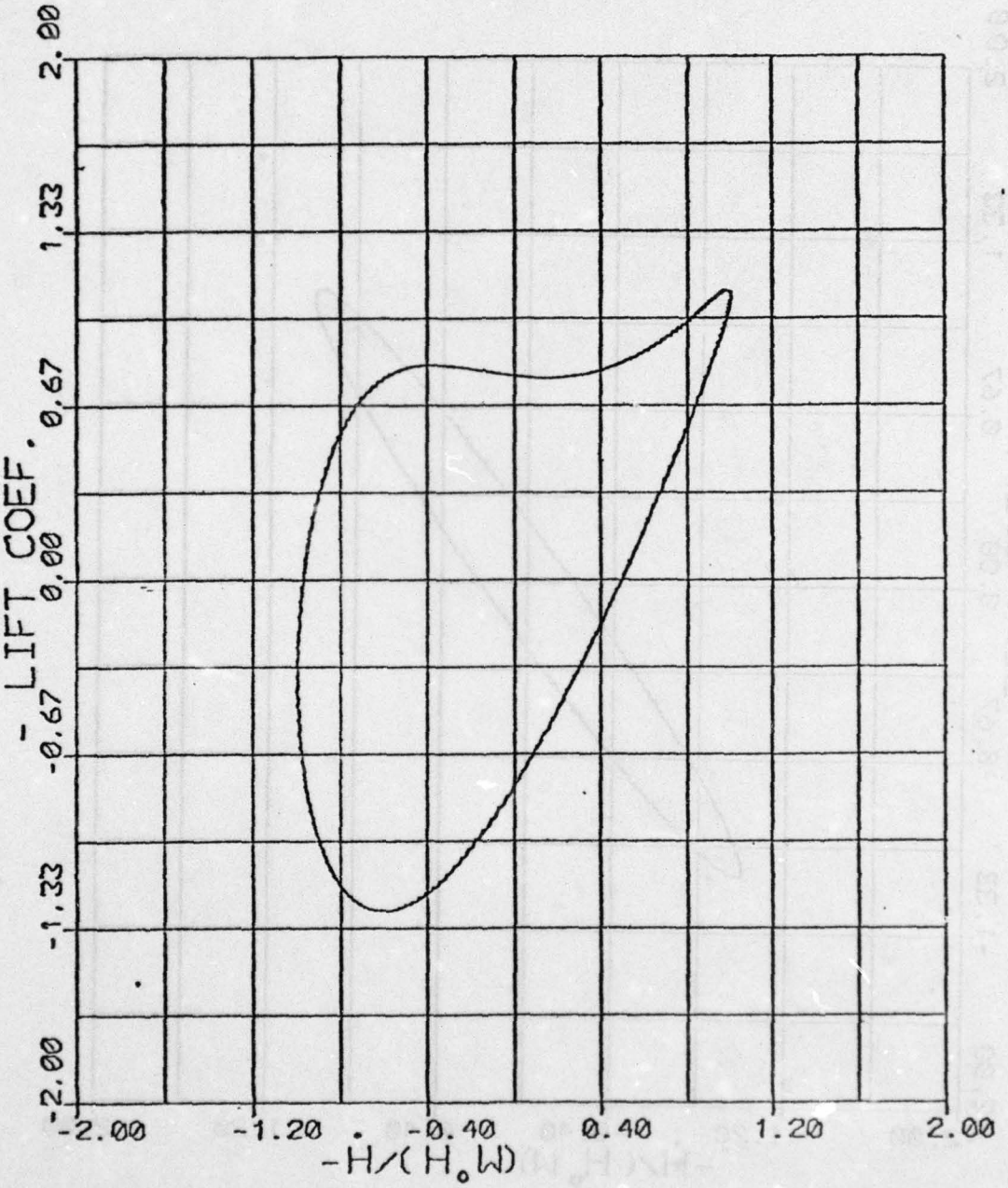

Fig. 12 - Lift coefficient as a function of dimensionless bending velocity with different reattachment point movement as compared to figures 8,10 and 11.

$S_1 = 1/3$ $K = 0.5$

$S_2 = 1/9$ $x = -\pi/2$

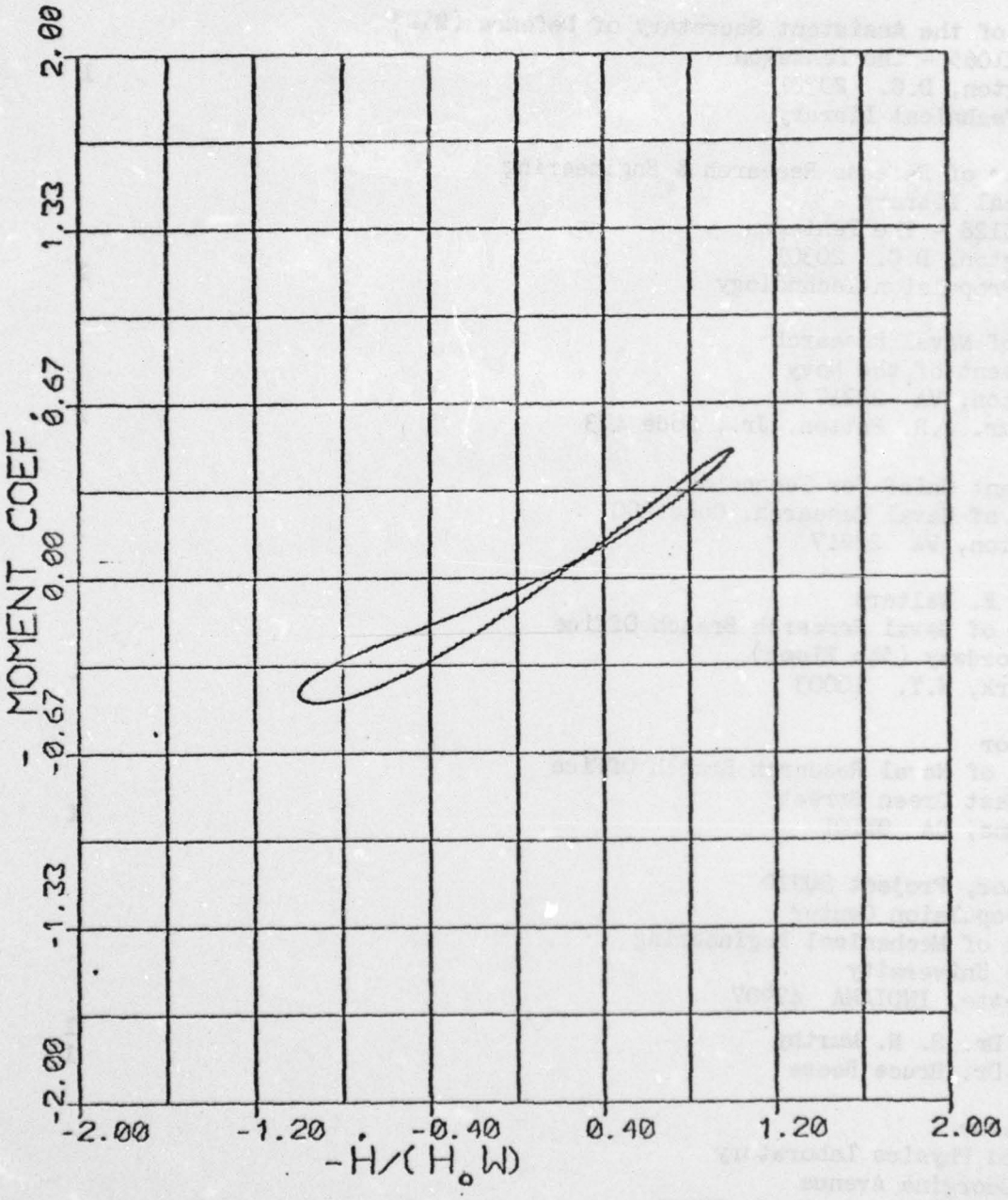

Fig. 13 - Example of moment coefficient loop for data of figure 8.

TECHNICAL REPORT DISTRIBUTION LIST

STEVENS INSTITUTE OF TECHNOLOGY CONTRACT N00014-76-C-0549 - NR 094-363

Recipient	No. of Copies
Defense Documentation Center, Bldg. 5 Cameron Station Alexandria, VA 22314	12
Office of the Assistant Secretary of Defense (R&D) Room 3E1065 - The Pentagon Washington, D.C. 20301 Attn: Technical Library	1
Director of Defense Research & Engineering Technical Library Room 3C128 - The Pentagon Washington, D.C. 20301 Attn: Propulsion Technology	1
Chief of Naval Research Department of the Navy Arlington, VA 22217 Attn: Mr. J.R. Patton, Jr., Code 473	2
Assistant Chief for Technology Office of Naval Research, Code 200 Arlington, VA 22217	1
Mr. F. E. Walters Office of Naval Research Branch Office 715 Broadway (5th Floor) New York, N.Y. 10003	1
Director Office of Naval Research Branch Office 1030 East Green Street Pasadena, CA 91101	1
Director, Project SQUID Jet Propulsion Center School of Mechanical Engineering Purdue University Lafayette, INDIANA 47907	
Attn: Dr. S. N. Murthy Dr. Bruce Reese	1 1
Director Applied Physics Laboratory 8621 Georgina Avenue Silver Spring, Maryland 20910 Attn: Library	1

Dr. Larry D. Mitchell
Associate Professor
Department of Mechanical Engineering
Virginia Polytechnic Institute and
State University
Randolph Hall
Blacksburg, VA 24061 1

Commander
Naval Air Systems Command
Department of the Navy'
Washington, D.C. 20361
Attn: Mr. R.R. Brown, AIR 330 1
Dr. H. Rosenwasser, Code 310C 1
Technical Library Div., Code 604 1

Commander
Naval Ship Systems Command
Dept. of the Navy
Washington, D.C. 20360
Attn: Mr. R.R. Peterson, Code 03413 1
Mr. C. Miller, Code 6146 1
Technical Library 1

Commander
Naval Ordnance Systems Command
Dept. of the Navy
Washington, D.C. 20360
Attn: Mr. B. Drimmer, Code 033 1

Commander
U.S. Naval Ordnance Laboratory
White Oak
Silver Spring, MD 20910
Attn: Library 1

Commander
Naval Weapons Center
China Lake, CA 93555
Attn: Technical Library 1

Bureau of Naval Personnel
Department of the Navy
Washington, D.C. 20370 1

Director
Ordnance Research Laboratory
Pennsylvania State University
University Park, PA 16802 1

Headquarters
Naval Material Command
Special Projects Office
Washington D.C. 20360
Attn: Technical Library 1

U.S. Naval Weapons Laboratory
Dahlgren, VA 22448
Attn: Technical Library 1

Naval Ship Research and Development Center
Annapolis Division
Annapolis, MD 21402
Attn: Library, Code A214 1

Officer in Charge
Naval Ship Engineering Center
Philadelphia Division
Philadelphia, PA 19112
Attn: Code 6700 1
Technical Library 1

Superintendent
U.S. Naval Postgraduate School
Monterey, CA 93940
Attn: Library, Code 0212 1

Director
U.S. Naval Research Laboratory
4555 Overlook Ave., S.W.
Washington, D.C. 20390
Attn: Technical Information Div. 6
Library, Code 2029 (ONRL) 6

U.S. Naval Oceanographic Office
Suitland, Maryland 20390
Attn: Library, Code 1640 1

Naval Missile Center
Point Mugu, CA 93041
Attn: Technical Library, Code 5632.2 1

Navy Underwater Sound Laboratory
Fort Trumbull
New London, CONN 06320
Attn: Technical Library 1

Commander
Air Force Systems Command
Andrews Air Force Base
Silver Hill, MD 20331 1

Commander
Air Force Office of Scientific Research
1400 Wilson Blvd.
Arlington, VA 22209
Attn: J. F. Masi 1

Commander
Wright Air Development Center
Wright-Patterson Air Force Base, Ohio 45433
Attn: AFAPL/RJ 1

Commander
Air Force Aero Propulsion Laboratory, TBP
Wright-Patterson Air Force Base
Dayton, Ohio 45433 1

Commander
Air Force Rocket Propulsion Laboratory
Edwards Air Force Base, CA 93523
Attn: WCLPS-1 2

Chief of Research and Development
Headquarters, Dept. of the Army
Washington, D.C. 20310
Attn: Dr. S.J. Magram
Physical & Engr. Div. 1

Army Missile Command
Research and Development Directorate
Redstone Arsenal, ALA 35809
Attn: Propulsion Laboratory 1

Commanding Officer
U.S. Army Research Office
Box CM, Duke Station
Durham, No. Carolina 27706
Attn: ORDOR-PC 1

Director
National Aeronautics & Space Administration
Headquarters
Washington, D.C. 20546
Attn: Division Research Information 1

National Aeronautics & Space Administration
Lewis Research Center
21000 Brookpark Rd.
Cleveland, Ohio 44135 2

Dr. R. H. Kemp
NASA-Lewis Research Center
MS 49-3
21000 Brookpark Rd.
Cleveland, Ohio 44135 1

Aerojet-General Corp.
P.O. Box 296
Azusa, CA 91702
Attn: Librarian 1

AiResearch Manufacturing Co.
9851 Sepulveda Blvd.
Los Angeles, CA 90045
Attn: Chief Engineer 1

Director
National Bureau of Standards
Gaithersburg, MD 20760 1

AVCO Corporation
Lycoming Spencer Division
652 Oliver St.
Williamsport, PA 17701 1

General Electric Co.
Engineering Dept.
Turbine Div.
Schenectady, N.Y. 12305 1

General Electric Co.
Aircraft Turbine Department
West Lynn, MASS 01905 1

General Electric Co.
Aircraft Gas Turbine Div.
Cincinnati, Ohio 45215
Attn: Manager of Engineering 1

Allison Division
General Motors Corporation
Detroit Diesel
Indianapolis, Indiana 46206
Attn: Director of Engineering 1

Solar Aircraft Co.
San Diego, CA 92101
Attn: Chief Engineer 1

United Technologies Corp.
Pratt & Whitney Aircraft Group
P.O.Box 2691
West Palm Beach, FLA 33402 1

United Technologies Corp.
Pratt & Whitney Aircraft Group
East Hartford, CONN 06118
Attn: Chief Engineer 1

United Technologies Corp.
Research Center
East Hartford, Conn. 06118
Attn: Director of Research 1

Varo, Incorporated
402 E. Gutierrez Street
Santa Barbara, CA 93101
Attn: K. J. Widiner 1

Westinghouse Electric Corp.
Steam Turbine Division
Lester Branch
Philadelphia, PA. 1

AVCO Lycoming Div.
550 So. Main St.
Stratford, CONN 06497
Attn: Division Library 1

SECURITY CLASSIFICATION OF THIS PAGE *(When Data Entered)*

REPORT DOCUMENTATION PAGE		READ INSTRUCTIONS BEFORE COMPLETING FORM
1. REPORT NUMBER	2. GOVT ACCESSION NO.	3. RECIPIENT'S CATALOG NUMBER
4. TITLE *(and Subtitle)* Research on the Flutter of Axial Turbomachine Blading		5. TYPE OF REPORT & PERIOD COVERED Technical Report November 1977 6. PERFORMING ORG. REPORT NUMBER ME-RT-77004
7. AUTHOR(s) Sisto, Fernando Tokel, Halil		8. CONTRACT OR GRANT NUMBER(s) N00014-76-C-0540
9. PERFORMING ORGANIZATION NAME AND ADDRESS Stevens Institute of Technology Castle Point Station Hoboken, N. J. 07030		10. PROGRAM ELEMENT, PROJECT, TASK AREA & WORK UNIT NUMBERS NR 094-363
11. CONTROLLING OFFICE NAME AND ADDRESS Office of Naval Research 207 West 24th St. New York, N. Y. 10011		12. REPORT DATE November 1977 13. NUMBER OF PAGES 38
14. MONITORING AGENCY NAME & ADDRESS*(if different from Controlling Office)*		15. SECURITY CLASS. *(of this report)* Unclassified 15a. DECLASSIFICATION/DOWNGRADING SCHEDULE

16. DISTRIBUTION STATEMENT *(of this Report)*

This document has been approved for public release and sale; its distribution is unlimited

17. DISTRIBUTION STATEMENT *(of the abstract entered in Block 20, if different from Report)*

18. SUPPLEMENTARY NOTES

None

19. KEY WORDS *(Continue on reverse side if necessary and identify by block number)*

Aeroelasticity; Nonstationary Aerodynamics; Vibration; Flutter in Cascade; Computational Fluid Dynamics.

20. ABSTRACT *(Continue on reverse side if necessary and identify by block number)*

The dynamic stall of an airfoil with leading edge bubble separation is analyzed. The stall flutter of turbomachine blading often involves periodic growth and collapse of such a bubble. The mathematical model representing the physical problem is presented. A flat plate undergoing harmonic oscillations with time dependent point of re-attachment is studied for the perturbed aerodynamic reactions & applications to the stall flutter problem.

DD FORM 1 JAN 73 1473 EDITION OF 1 NOV 65 IS OBSOLETE
S/N 0102-014-6601 |

SECURITY CLASSIFICATION OF THIS PAGE *(When Data Entered)*